3
Recent Advances in Column Technology

Ross Andrew Shalliker and Danijela Kocic

3.1
Introduction

Although it may not appear so, the HPLC column has undergone substantial changes in design since the first high-pressure packed columns were made. These early columns were manufactured using 10 μm ion-exchange particles and they were packed in a downward slurry process [1]. Since then, columns are typically packed with sub-3 μm particles, and we seem to be heading toward sub-2 μm particles, with even the 5 μm particles becoming less commonplace. With this downscale in particle size has come an increase in the number of theoretical plates per meter of column, which in the earlier days may have been generously estimated to be around 30 000–40 000 plates per meter to now typically on the order of 130 000 plates per meter for a 3 μm particle packed column, and nearing 180 000 plates per meter for 1.9 μm particle packed columns. This decrease in particle size has driven the need to increase the operational pressure of these columns, which in turn has led to the development of the UHPLC system. One added benefit of the advancements made in column technology was the design of chromatographic systems improved with greater attention paid to the extra column dead volume features of the instrument – but that is a different story. Columns are now typically 5 cm long rather than 25–30 cm; however, we still use just the same number, or even less, of plates in a given separation, some 40 years on.

In the past decade or so, the concept of pellicular particles was revisited, but in particle sizes less than 3 μm, most often 2.6 μm. The first of these reborn pellicular particles, or core–shell particles as they are termed, was the halo phase, but since then numerous types of core–shell particles have been commercialized, such as the Kinetex and Accucore columns. These types of particles have provided a higher separation performance, in part, because they pack more uniformly into a tube yielding higher numbers of theoretical plates [2]; typically, 250 000 plates per meter offer far greater efficiency than the fully porous particles.

Once silica was the primary stationary phase support, but now other types of ceramics are employed, for example, zirconia [3,4], titania [4], and alumina [4] which offer several significant benefits: pH stability, mechanical strength, and

Analytical Separation Science, First Edition. Edited by Jared L. Anderson, Alain Berthod, Verónica Pino Estévez, and Apryll M. Stalcup.

differing selectivity. Silica has also been developed as a hybrid phase incorporating organics into the support matrix [5]. Likewise, polymeric particles have found widespread use in ion chromatography and in gel permeation chromatography.

Selectivity is important in the development of separations and is, indeed, essential when dealing with complex samples. One needs only to glance through a supply catalog to testify the diversity of phases on offer. Such choice is particularly useful when developing two-dimensional separations, since for optimal performance each dimension should provide selectivity for the target species, ideally orthogonal retention behavior.

Monolithic columns have been developed in silica and polymeric forms. Their advantage is the increased bed permeability [6], which allows for higher speed in separation performance. Their disadvantage is that the separation performance is poorer than that of the particle packed columns. Further development work is required here. While monoliths are an important aspect of column technology, they will not be discussed further here since an entire chapter could be devoted to monoliths. Indeed, Guiochon [6] comprehensively reviewed monoliths in 2007, and the reader can refer to his works for more information, albeit, an update is soon warranted.

Perhaps, the most stagnant region of this development has been in the design of the container that houses the stationary phase. Largely, this container is a tube whose purpose is to house the particles in a tightly packed order and allow the solvent to traverse efficiently through the bed. Some novel design strategies were constructed in an effort to improve the solvent transport, namely, radial compression columns [7], which have soft walls that could be pressurized and bent around the particles to overcome wall effects (this will be discussed in more detail later). However, the radial pack column could not gain market acceptance and its use faded. Some specialized column formats have been tested, for example, an injection technique known as central point injection [8], where a needle is inserted into the bed at the inlet and the sample is introduced and restricted during migration in the radial central region of the column – the so-called "infinite diameter column" [8]. Its use in real-world applications was, however, limited. Similarly, in an attempt to overcome the wall effect, end-point detection processes were investigated [9–12], where instead of the bulk eluent passing through a detection source being used to collect chromatographic data, a localized detector is employed which is located usually in the central region of the outlet end of the column, such that the detector sees just the solute species that migrate through the radial central region of the column. This process greatly improves the separation performance, but it is difficult to implement in an automated and general run-of-the-mill laboratory. Hence, it has not found acceptance in commercial practice.

More recently, a new design concept in HPLC columns, referred to as active flow technology (AFT) [13–16], is undergoing development, and this is the focus of this chapter. In order to understand this design feature, we first need to understand how columns are packed. Hence, we will begin our discussion by summarizing the column packing techniques and then we will evaluate factors that prove to be detrimental to column performance.

3.2
Column Packing: Downward Slurry Packing

Downward slurry packing methods dominate commercial manufacturing processes, for at least analytical scale columns. However, manufacturers treat their packing protocols as closely guarded secrets. Furthermore, there are no generic methods for column packing since different types of materials demand different packing conditions, even to the point whereby not all types of C_{18} columns can be successfully packed using the same packing method. All this indicates that column packing processes remain incompletely understood. The particle size and the size distribution further complicate the process.

The general principle of downward slurry packing is, however, relatively straightforward. In the first instance, a suitable solvent must be identified that allows the particles to be dispersed, avoiding the formation of agglomerates. The particles are stirred in this solvent until completely dispersed: ultrasonication should be employed to remove trapped air from within the particle pore structure. Next, a suitable packing or pushing solvent needs to be identified. The purpose of this solvent is to carry the particles into the column at high velocity and subsequently consolidate the particles tightly in the column tube. As a guide, acetone generally serves as a useful dispersive solvent for C_{18} particles and methanol as a packing solvent; although this combination does not work for all C_{18}s, it is at least a useful starting point. These solvents are likely not suitable for all types of bonded phases.

A typical example of column packing equipment used for downward slurry packed columns is shown in Figure 3.1. An air-driven fluid pump (a), capable of delivering solvent at high pressure and high volumetric flow rates, is usually employed. The piston volume of this pump should be small so as to avoid large-pressure fluctuations during piston chamber refill, or the piston volume

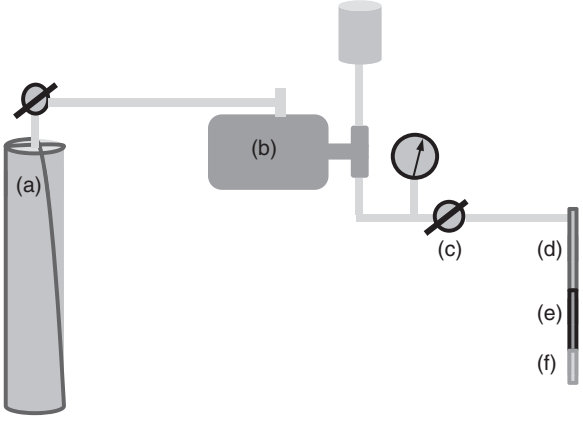

Figure 3.1 Schematic diagram of a typical downward slurry packing system: (a) high-pressure gas-driven fluid pump, (b) compressed gas, (c) gate valve, (d) slurry reservoir, (e) column blank, and (f) sacrificial column blank.

should exceed that of the volume required to pack the column entirely so as to avoid any refill at all. The latter is technically more difficult to achieve due to the rigors associated with high-pressure and high-volumetric flow rates, but this depends on the column's internal diameter. The pump is driven by compressed air (b).

Pressure from the pump is built up against a gate valve (c), typically at around 7000 psi. To initiate the packing process, this gate valve is opened rapidly. Below the gate valve, there is a slurry reservoir (d), the column (e), and a sacrificial outlet section (f). Prior to loading the slurry reservoir, the column blank and the sacrificial outlet section are filled with a displacement solvent. Ideally, this solvent should have a similar density to that of the slurry, although obtaining a solvent to match is difficult, especially one that is safe and environment-friendly to use. Although not perfectly matched to the typical slurries used in reversed phase columns, dichloromethane serves as a suitable choice. The purpose of using this solvent is to prevent the premature settling of particles within the column blank prior to the initiation of high-pressure and high-velocity fluid flow. The slurry will remain suspended above the displacement solvent through the duration of the packing process [17]. The particle slurry is added to the slurry reservoir (d) carefully, but quickly, capped, and then the packing process begins. Upon the application of pressure to the slurry reservoir, the slurry travels into the column blank more or less as a discrete plug, which gradually compresses like a spring as it moves through the tubing [17]. Once the column cylinder is filled with particles, the packing solvent should be passed through the column bed until such a time that the pulsations on the packing pump reach a constant time interval.

3.3 Column Bed Heterogeneity

It is now well understood that packed chromatographic beds are heterogeneous, both in the axial and in the radial directions. While heterogeneity in the axial direction leads to a general broadening of an elution profile and a loss in efficiency, it is radial heterogeneity that is a far more serious contributor to the loss in column performance, since radial heterogeneity leads to a distortion of the elution profile, from the ideal cylindrical plug flow to a parabolic, cup-like elution profile. In the following discussion, the terms "radial" and "axial" heterogeneity have been evaluated separately, although there are commonalities in the cause of each aspect of heterogeneity.

3.3.1 Axial Heterogeneity

Even in modern HPLC columns, with the exception of core–shell particles, reduced plate heights lower than 2 are rarely reported. There are a few works that have reported h values near unity [18–21], but these were especially

prepared columns and operated under strictly controlled conditions, certainly not suitable for routine applications. Perhaps, we have reached our limits with respect to how well spheres, whether monodisperse or not, can be physically packed inside a column, since inside the column there are significant variations in the packing density and hence local differences in the void space.

One important aspect of the column packing process that leads to column packing irregularities is friction, which can affect both axial and radial homogeneity of the column bed. First, however, we will consider how friction is a contributing factor to axial heterogeneity. One analogy that describes very well this effect was articulated by Jaeger, Nagel, and Behringer [22]. The authors related the close packing of particles to the "close" packing of cars in parking spaces inside a parking lot. In this parking lot, there are no assigned spaces and the aim is to completely fill the lot with uniformly parked cars. If, however, one car in the lot is poorly parked, occupying more than an equivalent single space, then in order for another car to park in this lot, the poorly parked vehicle must be moved and parked in a more orderly fashion. To do this, many cars must be moved at the same time, since other cars have effectively parked in a fashion dictated by the poorly parked car. Particles undergoing packing in a cylindrical tube behave in the same manner; once a particle is poorly packed and other particles are consolidated around this particle, they are more or less fixed in place. A uniform bed may build up beyond their space, but their poorly packed presence has created a void space within the tube. In order for this void space to be filled and additional particles added to the column, many particles must be reordered. While on an individual basis the frictional forces between particles may be insignificant, when taken on a whole across the entire column, there is an enormous resistance to particle movement. Hence, how these particles enter the column and are then consolidated is critically important to the quality of the packed bed. For interest, however, the reader can refer to reference [23], which shows that these small individual friction forces between particles can be overcome using ultrasonic radiation applied to columns running very low-viscosity mobile phases at low flow rates.

Understanding the significance of the *parking lot effect* is an important consideration when understanding how columns are physically prepared. In Section 3.2, the downward slurry packing process was discussed, and this technique is largely used to pack analytical scale columns. When doing so, pressure is built up against a gate valve and then rapidly released to drive the particles from the slurry reservoir into the column tubing. The particles enter the column tube at very high velocity, and the bed progressively builds up. If packing is undertaken at constant pressure, the flow velocity must, therefore, decrease as the bed length increases. Hence, particles on the outlet section of the bed have traveled at a higher velocity than particles at the inlet section of the bed. Systematically, therefore, there is a variation in the bed density along the axial direction of the column [24]. In a 30 cm bed, the bed density may increase by as much as 7% from the inlet to the outlet [24]; even on a 10 cm bed, the average bed density for the outlet 5 cm section of the column was observed to be 4% higher than the inlet 5 cm section [24].

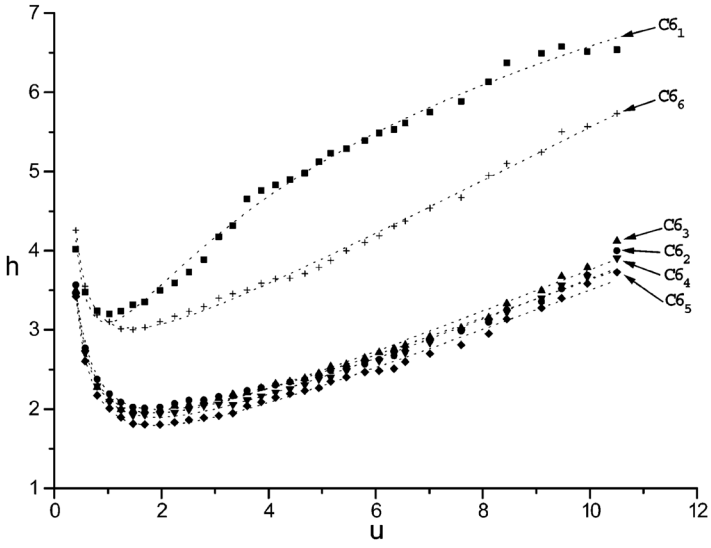

Figure 3.2 Plot of HETP curves for six, 5 cm sections of 30 cm column. (Reproduced with permission from Ref. [24].)

More serious than this variation in bed density is, however, the uniformity of the packing material. At the column inlet, where the bed is least dense and the packing material is not protected from the high-velocity fluid flow stream (since there is no frit), the column bed is poorly packed. Channeling as a consequence of the unprotected bed surface being exposed to the flow stream may be a factor in the poor performance. The HETP curves shown in Figure 3.2 illustrate this phenomenon. The column labeled as $C6_1$ is the inlet 5 cm section of a 30 cm bed (isolated from the 30 cm section using techniques described in reference [24]). The HETP curve reflects the poorest separation performance of any of the sections within the bed.

At the outlet section of the column, that is, a 5 cm section extracted from a 30 cm bed [24], the packing density is at its highest, although the HETP curve (Figure 3.2) does not reflect that of the best performing section of the column. Hence, a high bed density does not necessarily reflect a better packed bed. To understand why this section of the column is poorly packed, we need to appreciate the packing process itself. Packing commences following the rapid opening of the gate valve. Studies on glass column have shown that during the transportation process of slurry to the column, the slurry moves as a plug and compresses like a spring [17]. The packing pump used to pack the column in reference [24], the HETP curves for which are shown in Figure 3.2, had a stroke volume of 11 ml. Approximately, three pump strokes were required before the bed was fully built within the column. During refill of the pump piston chamber, a pressure pulse was established–around 2000–3000 psi. After these initial pump pulsations, the fluctuations decrease by a factor of 10.

As the bed builds within the column housing, the velocity of fluid decreases to maintain constant pressure. This means that the particles that impinge upon the outlet frit of the column blank do so with the greatest momentum of any other particle impinging upon the bed. This results in a decreasing bed density from the outlet to the inlet of the column, and leads to the question why the mass of the packing material was greatest in the outlet section and least in the inlet section. This was observed in the columns packed in reference [24], the HETP curves for which are shown in Figure 3.2. One might consider that the greater the packing density, the less voids within the bed, and hence the better the column efficiency. Yet, the HETP curves do not support this assumption. Rather, the efficiency of this outlet section of the column was very poor. The poor performance of this section is likely to arise from the initial two–three pumping strokes in which the pressure change in the column is on the order of 2000–3000 psi. During these pulsations, the bed at this point in time has not yet been consolidated and during these first pump strokes, the bed undergoes a rapid succession of large expansions and compressions. This causes the particles in the outlet section to move upward from the frit in a manner similar to the fluffing of a finely divided solid in a vacuum that is rapidly released to atmospheric pressure. Even a minor disturbance here is catastrophic to the bed quality, since these particles cannot return to their original position within the bed with the same degree of momentum and as such voids are established [24]. Once these voids are established, they remain fixed in place since the bed builds up quickly on top of these particles. To remove these voids, the parking lot effect must come into play.

Once the outlet and inlet sections of the column have been removed, the remaining internal sections of the column are relatively homogeneous, with respect to the axial direction [24] (Figure 3.2).

3.3.2
Radial Heterogeneity and the Wall Effect

The effects of radial bed heterogeneity on column efficiency are far more serious. The details of radial bed heterogeneity were recently reviewed [16], and as such only a brief account of the bed heterogeneity is considered here. Knox, Laird, and Raven [8,25], Golay [26], and Eon [7] were the pioneers who investigated the column bed heterogeneity. These early works were undertaken in dry packed beds and independently they identified that the flow velocity of the mobile phase in the radial column center was different from the flow velocity of the mobile phase near the wall. In the dry packed beds of reference [8], the flow velocity increased as the wall was approached, and at the same time, the reduced plate height increased from the radial center ($h = 1.7$) toward the wall ($h = 4.7$). It was these early studies of Knox, Laird, and Raven [8,25] that paved the way for the notion of a "wall effect." Eon [7] then studied in more detail the "wall effect" and in particular focused attention on minimizing wall effects by using soft-walled columns or radial compression columns as they are more commonly known.

Eon's study [7] was one of the earliest that described the concept of these radial compression columns.

Later, Baur and Wightman [9] studied the column bed heterogeneity in slurry packed columns, the particle size of which was 3 μm. They used an end-column microelectrode that could be precisely positioned at various radial locations. They were able to show that the reduced plate height increased significantly as the wall was approached; in the radial column center, the reduced plate height was 1.9, but near the wall, the reduced plate height was 4.2. This finding was similar to that of Knox and Parcher [8], but there was one significant difference: the flow velocity in the slurry packed columns was ~5% higher in the radial column center than near the wall.

Later, studies by Farkas *et al.* [10–12] investigated the radial column bed heterogeneity. Like Baur and Wrightman [9], they used microelectrodes [10] at the column outlet to observe how the flow velocity and column efficiency varied as a function of the radial location. They also used fluorescence detection to improve spatial resolution [11,12]. They found that the velocity was systematically lower near the wall than in the radial center of the column, irrespective of the particle diameter, and the efficiency was highest in the radial column central region of the bed. The magnitude in the difference between the flow velocities through the center compared to the wall region decreased as the flow rate decreased, until it became effectively negligible when the column was operated at its optimal flow velocity.

Tallarek and coworkers used magnetic resonance imaging to evaluate the column bed heterogeneity [27–30], and like Eon their studies focused on radial compression columns. In columns packed with large irregular particles, localized variations in radial packing density (as much as 30%) were observed. When the column was radially compressed, the radial packing density varied even more. Columns packed with smaller spherical particles (6 μm) were in contrast effectively homogeneous, with variation across the column being less than 1%.

The on-column matched refractive index detection process developed by Shalliker, Broyles, and Guiochon [31] was also used to study a variety of flow phenomena that detailed heterogeneity in the radial flow of the mobile phase through slurry packed beds. The most important outcome of these studies was the physical proof that detailed the wall effect [32]. They showed for the first time that there were two wall effects: the first wall effect, being a consequence of the column and particle geometry, neither the rigid particles nor the rigid column wall could bend to accommodate the other. As a consequence, the void space next to the wall was the greatest within the column. Hence, in this region of the packed bed, the permeability was at its highest. So, the flow velocity here was the highest; in fact, they observed a 37% increase in the flow velocity at the wall compared to the column radial center. The second wall effect was a result of the packing density increasing gradually as the wall was approached (but not at the wall). Near the wall, the flow velocity was the slowest, since the packing density was the greatest. In the radial central section of the bed, which extended from the radial center to around two-thirds of the column internal diameter, the

flow was relatively homogeneous. The solute migration efficiency was at its highest in this central region, decreasing as the wall region was approached. Subsequently, these studies verified the general findings of Baur and Wightman [9] and Farkas *et al.* [10–12] and provided a conclusive proof of bed heterogeneity with a detailed description of the wall effect.

3.4
Active Flow Technology: A New Design Concept in Chromatography Columns

In an effort to overcome column bed heterogeneity, at least with respect to radial heterogeneity and wall effects, a new design concept in column technology was developed. This technology has been referred to as AFT [13–16] and comprises a suite of columns that offer various performance attributes beyond the capabilities of conventional HPLC columns. Two of the most important columns within the AFT suite are (i) the parallel segmented flow column (PSF) [14,16] and (ii) the curtain flow column (CF) [13,16]. Both of these columns provide a distinct advantage over conventional columns and their design features and mode of operation will now be discussed in detail.

3.4.1
AFT Columns: Parallel Segmented Flow

Figure 3.3 is an illustration of a parallel segmented flow chromatography column, which has been designed to separate the flow streams that migrate in the wall region from the radial central region of the column [16]. In that way,

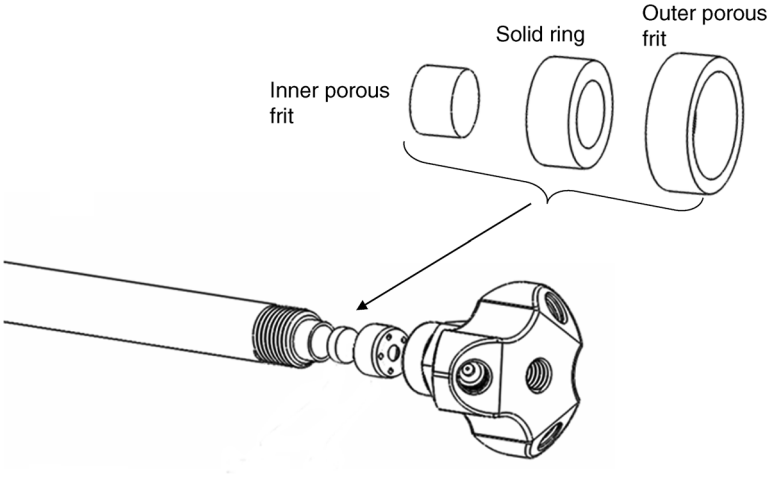

Figure 3.3 Illustration of the AFT end fitting, that is, the parallel segmented flow fitting, showing a sketch of the outlet frit and the outlet end fitting. (Reproduced with permission from Ref. [14].)

inefficiency associated with wall effects and bed heterogeneity is overcome. The design of the column consists of an annular frit whereby the central portion of the frit is separated from its outer portion by a solid PEEK ring. This frit prevents cross dispersion of solute between the radial central region of the migration zone and the wall or peripheral zone of the column. The frit is housed in an outlet fitting that has multiple exit ports: a central port that directs the flow from the radial central region of the column and a peripheral port or ports that capture the flow eluting from the outer annulus or wall region of the frit. The purpose of this outlet fitting is to segment the flow into two portions: (1) the central portion and (2) the peripheral or wall region portion. The flow from either of these ports can be processed further, that is, passed through a detector or the sample collected in a fraction collector. The segmentation ratio (central flow : wall flow) is easily adjusted by regulating the pressure in any of the respective outlet ports. In fact, differential flow rates can be established through any of the exit ports, whether it is the two-port end-fitting design or the four-port end-fitting design, or any other multi-port design. Another benefit of the multiport end fitting is that it enables multiplexed detection processes to be developed that enhance the analysis of complex samples [33–35].

A key to understanding the benefits of active flow technology is the realization that segmentation of the outlet flow from the chromatography column creates what is in effect a "virtual" column inside the physical column [15]. Solutes that migrate through the radial central region of the column exit the column via the radial central exit port, that is, they traverse the bed through the virtual column and migrate without any interaction with the column wall. The virtual column is in effect a wall-less column. The virtual diameter of this wall-less column can be tuned, perhaps, either to suit the needs of the detection mode [15,36] or to influence the level of column efficiency [14,15] or sensitivity [14]. For example, if the physical internal diameter of the parallel segmented flow column is 4.6. mm, and 21% of the flow eluted from the radial central outlet port, then effectively a virtual column is established, which has a virtual internal diameter equivalent to 2.1 mm. Likewise, if 43% of the flow were allowed to elute through the radial central exit port, then a virtual 3.0 mm i.d. column would be established. It is a very simple task to tune this segmentation ratio, and column efficiency and sensitivity both depend on the segmentation ratio. More details regarding this will follow as we discuss the separation performance.

3.4.2
AFT Columns: Curtain Flow

Curtain flow chromatography columns [13] utilize the same outlet fittings as detailed in Figure 3.3 for the PSF columns. But, curtain flow columns differ from the PSF columns because the multiple port end fitting and frit are located at both the column inlet and the column outlet. The sample is introduced into the radial central region of the column through the radial central inlet port. Mobile phase is introduced into the column through both the radial central inlet port and the

peripheral port(s). This can be achieved by either splitting the flow prior to the injector or by using two pumping devices, one for the central flow and the other for the peripheral flow [37]. On a 4.6 mm i.d. column, the ratio of the central flow to the peripheral should be somewhere in the vicinity of 35 : 65 [13] for best performance. Since the sample enters the column via the radial central inlet port, it then enters into the central porous region of the annular frit. The impermeable ring located inside the inlet frit prevents the sample from dispersing through the frit to the wall. Once the sample load enters the column, the peripheral flow of mobile phase then further inhibits the diffusion of solute to the wall, effectively establishing a curtain flow environment. Solutes then migrate through the column with no interaction with the wall. The principles of the infinite diameter column are thus applied. The outlet segmentation ratio can, however, be adjusted to tune the internal diameter of the virtual column so as to optimize efficiency and sensitivity, with respect to the detection mode being utilized.

3.4.3 Performance of AFT Columns

3.4.3.1 Sensitivity

Because packed column beds are not perfectly homogeneous, and that the sample is not uniformly distributed across the inlet section on the column, the AFT end fitting and frit assembly does not function in the same manner as the post-column flow stream splitting. The heterogeneity of the packed bed generates

Figure 3.4 Photograph illustrating a regular injection profile through a glass packed column. (Reproduced with permission from Ref. [38].)

flow profiles that resemble partially filled bowls [38], similar to that shown in Figure 3.4 (a photograph of a band profile inside a glass column operating in a matched refractive index system according to reference [38]). When viewed from the trailing edge of the band profile, it is apparent that the band is partially hollow. The post-column flow stream splitting samples the entire band profile equally, that is, the concentration of the solute in either portion of the split that emanates from a post-column splitting system will be in proportion to the split ratio. However, the segmented outlet fitting on an AFT column samples the inner core region of the profile separately from the outer core region of the profile, effectively heart cutting the radial central region of the band, resembling a doughnut. The concentration of the radial central portion is not equal to the concentration of the outer core region because (1) frits do not distribute the sample uniformly across the head of the column [39–41] and (2) the column is less efficient near the wall [32], so band broadening is greater near the wall and thus the sample is diluted. Hence, even when small portions of the flow are sampled from the radial central outlet section of the column, the concentration response on a detector can be as high as, or even higher than, the larger volume peripheral portion of the flow, or for that matter, the entire portion of the flow eluting from the exact same format conventional column carrying the same solute loading. This is clearly shown in Figure 3.5, where it can be seen that at a segmentation ratio of 15% through the column central exit port, there is the same sensitivity in UV detection as 100% of the sample eluting from a conventional column [14], such is the significance of the radial heterogeneity and the bowl-shaped elution profile. Another important aspect from this data is that the band volume is decreased in the exact proportion to the outlet segmentation ratio, and this has major benefits when utilizing flow sensitive detectors, such as the mass spectrometer (to be discussed later).

Sensitivity in detection can be boosted in CF column mode, because the sample is restricted to the radial central region of the bed. In CF, sensitivity with UV detection is almost three times higher than conventional columns [37] as shown by the chromatographic trace in Figure 3.5. Even greater gains in sensitivity are achieved when CF columns are used with MS detection [36]. In some instances, almost 70-fold gains in S/N responses have been observed as a consequence of a substantial reduction in the baseline noise when AFT columns are used [36]. The noise response has been shown to be solute dependent, with the largest variations arising from separations undertaken on conventional columns [36], rather than the AFT columns. For example, an illustration of the noise response is shown in Figure 3.6a for extracted ion chromatograms of phenylalanine and Figure 3.6b for extracted ion chromatograms of methionine. Note the noise response for these two amino acids on the AFT columns remains almost constant, but is highly variable for the data collected on the conventional columns [36].

3.4.3.2 Efficiency

When comparing the efficiency of AFT columns and conventional columns, two sets of reference points need to be established. The first is a comparison between

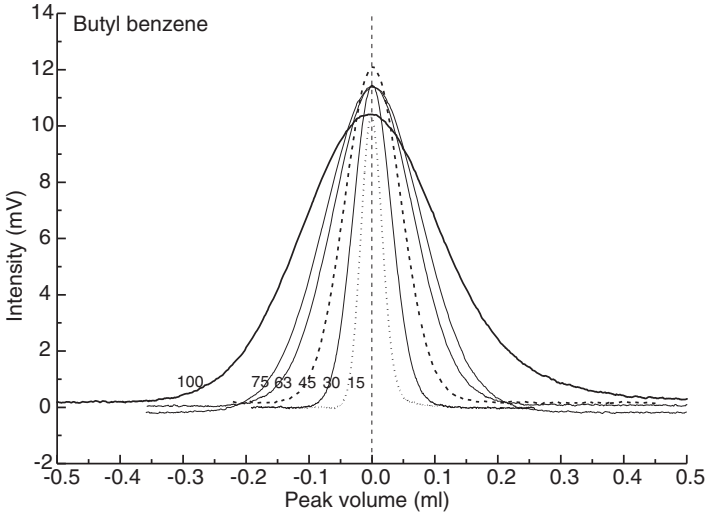

Figure 3.5 Band profiles of butyl benzene eluting from the column operating in a normal mode (100) and segmented modes 75–15% solvent exiting via the central port as marked. Bandwidth expressed in units of volume. Mobile phase 30/70 water/methanol, flow rate 1.1 ml/min, injection volume 2 µl, and detection 250 nm. (Reproduced with permission from Ref. [14].)

AFT columns and conventional columns whereby they both have the same physical internal diameters; of course, the particle size and length also remain constant. The second reference point is the comparison between a conventional column that has the same physical internal diameter as the internal diameter of the virtual column that is established by the AFT column. The reason this second reference point is required is that there is a comparison made at constant linear velocity through the flow cell of a detector between the two column sets. When the flow is segmented at the column outlet on an AFT column, the flow rate through the detector is reduced and depends on the segmentation ratio; hence, the residence time in the detector is increased. Thus, when making comparisons between the virtual column and the conventional column with a matching internal diameter, flow rates and detector residence times are the same. This provides for an even comparison, with respect to the flow rate and to the volume of an elution profile. The efficiency of the AFT column is generally underestimated by 7–10% because of the increase in residence time within the detection flow cell.

The efficiency of an AFT column depends on the segmentation ratio [14,15]. At very low segmentation ratios, post-column dead volume contributions become more significant and this decays the efficiency gains obtained, relative to a conventional column with the same physical internal diameter as the AFT column. Albeit, the efficiency of the AFT column remains very much higher than the comparative conventional column that has the same internal diameter as the

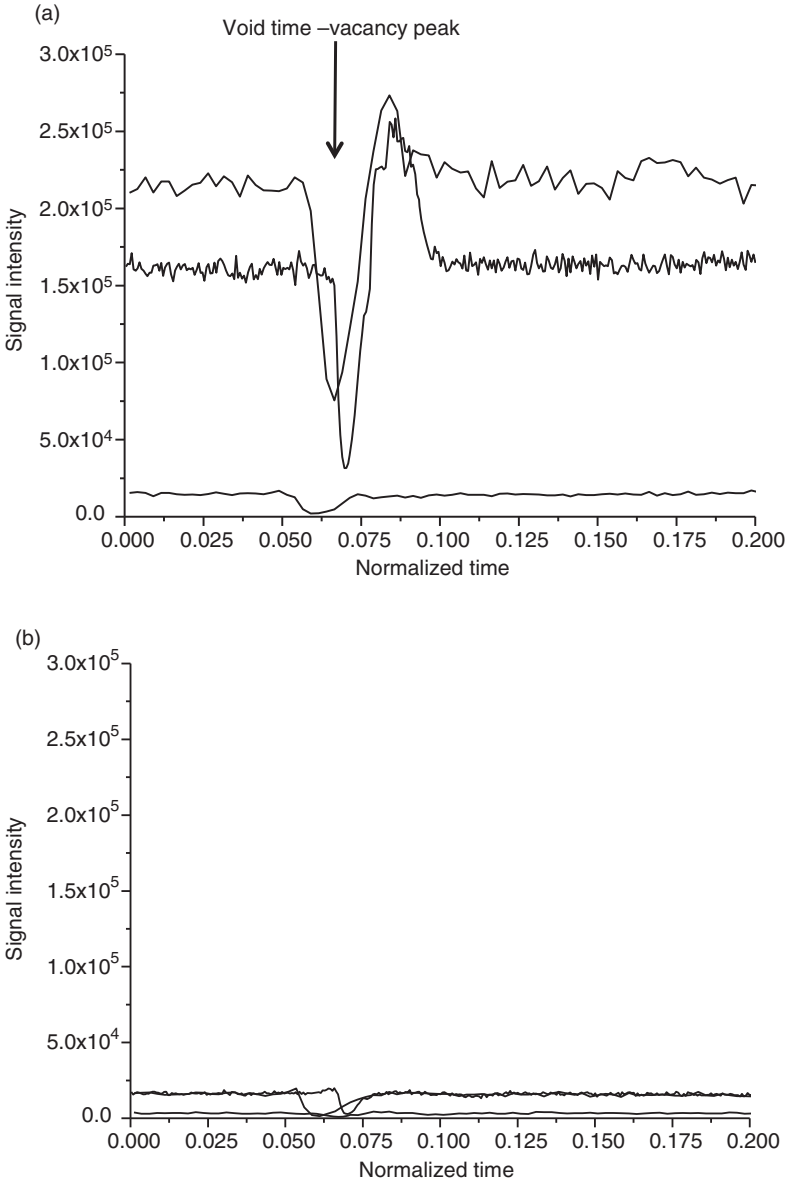

Figure 3.6 (a) Plots showing the noise contributions for each of the three columns for extracted ion chromatograms of methionine. Note the time axis is expressed as a fraction of the total run time, that is, normalized time between 0 and 1. Each plot represents the first 20% of the total time. (i) Curtain flow column, (ii) 2.1 mm i.d. conventional column (bold), and (iii) 4.6 mm i.d. conventional column. (Reproduced with permission from Ref. [36].) (b) Plot of the baseline noise response for the EIC for *m/z* 150 (methionine) on the same scale as that for phenylalanine in Figure 3.6a. (Reproduced with permission from Ref. [36].)

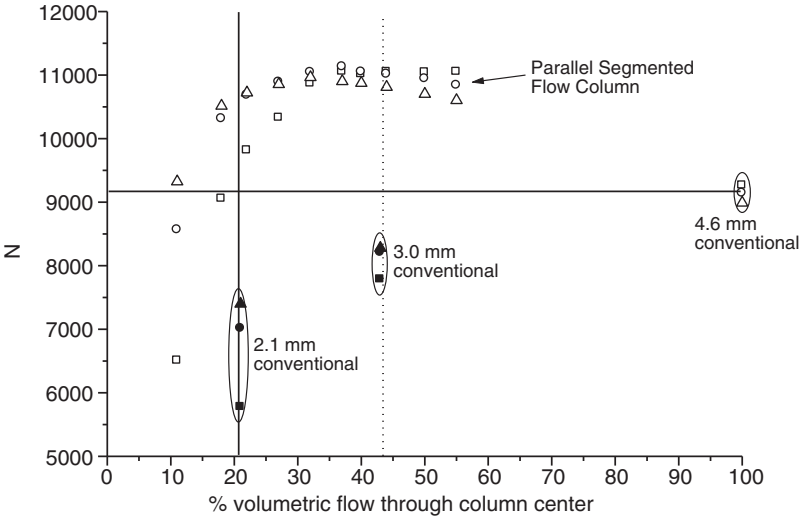

Figure 3.7 Comparison in *N*-values obtained on the 4.6 mm i.d. parallel segmented outlet flow column, the 4.6 mm i.d. conventional column, the 3.0 mm i.d. conventional column, and the 2.1 mm i.d. conventional column. Test solutes: toluene (squares), propylbenzene (circles), and butylbenzene (diamonds). All columns were packed with 5 µm Hypersil Gold particles in formats of 2.1, 3.0, and 4.6 mm i.d., and each column was 100 mm in length. (Reproduced with permission from Ref. [15].) Note the data obtained on the 2.1 mm and 3.0 mm i.d. columns are centered on the 21% and 43% volumetric flow positions to correspond to the equivalent flow through the 4.6 mm i.d. column at that specific segmentation ratio.

virtual column established by the AFT column [15]. Figure 3.7, for example, shows the magnitude of typical gains in efficiency: AFT versus a variety of conventional columns [15]. Gains in *N* were as great as 70%.

The efficiency gain of an AFT column is also length dependent. Smaller gains are apparent using longer columns, presumably because the solute species has greater opportunity to migrate as part of its elution time in the wall region [42]. For columns packed with 5 µm particles, the optimal length was on the order of 15 cm [42], where gains in efficiency were by as much as a unit value in the reduced plate height term. While for columns packed with 3 µm particles, the gain in efficiency decreased as the column length increased for columns between 3 and 10 cm in length. However, the gain in efficiency for the 3 µm particle-packed columns was far greater than for the 5 µm particle-packed columns. On the 3 cm column, for example, gains in efficiency were by as much as 4 reduced plate height units and about 1.8 reduced plate units on the 10 cm column.

A very significant benefit of the AFT columns is that the efficiency gain when compared to conventional columns increases as the flow rate increases, and this favors high-throughput applications. The HETP curves in Figure 3.8, for

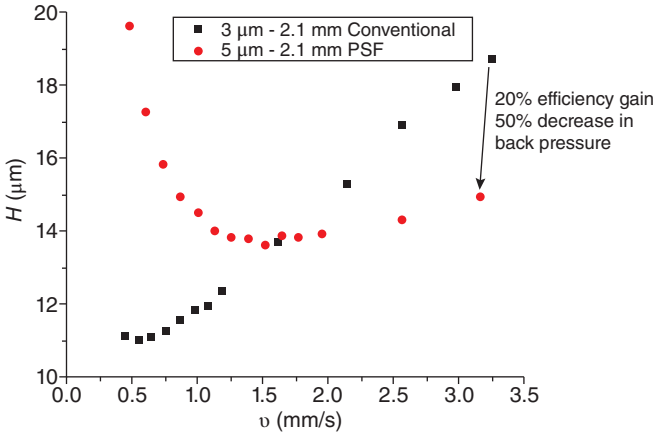

Figure 3.8 HETP curves on 50 mm × 2.1 mm format columns: the conventional column (squares) was packed with 3 µm Hypersil Gold particles and the PSF column was packed with 5 µm Hypersil Gold particles. (Reproduced with permission from Ref. [43].)

example, show that a 5 µm particle-packed AFT column, with a virtual internal diameter of 1 mm outperforms a 2.1 mm internal diameter conventional column packed with 3 µm particles when the flow velocity exceeds ~1.6 mm/s [43]. When the 3 µm particle-packed column has reached its operational pressure limit, the 5 µm particle-packed AFT column has 20% more theoretical plates and functions at half the back pressure [43].

3.4.3.3 Speed

Perhaps, the most impressive benefit of AFT columns can be seen in ultrahigh-speed separations, especially when these are coupled to flow-rate-limited detectors, such as the mass spectrometer. In general, the HPLC process limits the throughput of HPLC–MS analyses because of the time required to undertake a separation in the LC step. The MS process limits the throughput of the HPLC–MS assay because of the limited volume of the solvent that can be processed by the MS. This is essentially the reason why HPLC–MS is undertaken using narrow bore columns – higher throughput in the LC, but without overloading the volume capacity of the MS.

Narrow bore AFT columns (2.1 mm i.d.) provide for very high efficiency at very high linear velocities compared to the conventional columns. The HETP curves in Figure 3.9 show the efficiencies of conventional and AFT columns over a very wide range of linear velocities. The upper velocity tested corresponded to a flow rate of 2 ml/min. On the conventional column, 1000 theoretical plates were obtained, but on the AFT column operating with a 21% segmentation ratio, 2000 theoretical plates were obtained; effectively, the 5 µm PSF column functions from an efficiency perspective as if packed with 2.5 µm particles, but with the pressure of a 5 µm particle-packed column.

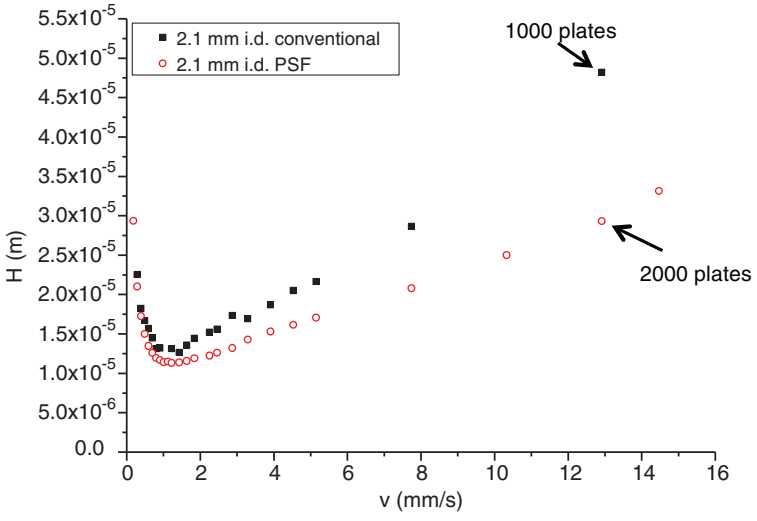

Figure 3.9 HETP curves on 50 mm × 2.1 mm format columns both packed with 5 µm particles (Hypersil Gold). Test solute: propylbenzene, 40/60 water/methanol mobile phase. Injection volume: 1 µl. UV detection at 254 nm.

Given these gains in efficiency, and the fact that the solvent load to the MS detector is greatly reduced, there is an exceptional potential for very high-throughput operations. We have, in fact, named this technique "pulsed direct injection" HPLC–MS. This refers to a separation technique with HPLC and MS, whereby the process acts in a manner similar to direct injection into the MS (in the absence of a column); however, this direct injection is pulsed, by virtue of the fact that an AFT column is incorporated into the scheme, but it operates in a manner such that it has virtually no impact on the processing speed. It does, however, establish a "pulse" into the assay, the frequency of which is dictated by the injection cycle time. The extracted ion chromatograms in Figure 3.10 illustrate nicely this technique. In this separation, a 50 mm × 2.1 mm i.d. PSF column, packed with 5 µm particles, was employed, and the flow rate was 3 ml/min, resulting in a cycle time (injection to injection) of 18 s, 6 s of which was the time required to inject the sample; the separation was completed in 12 s. In Figure 3.10, there are 10 replicate injections of a three-component sample: acetaminophen, caffeine, and piroxicam. We deliberately chose conditions such that acetaminophen and caffeine coeluted in the HPLC separation but were separated by the triple-quadrupole MS. The precision in area quantification was excellent: 2.4% for acetaminophen, 1.2% for caffeine, and 1.4% for piroxicam. This type of analytical technique shows a great promise in processes that involve reaction monitoring, where assay speed and selectivity is essential.

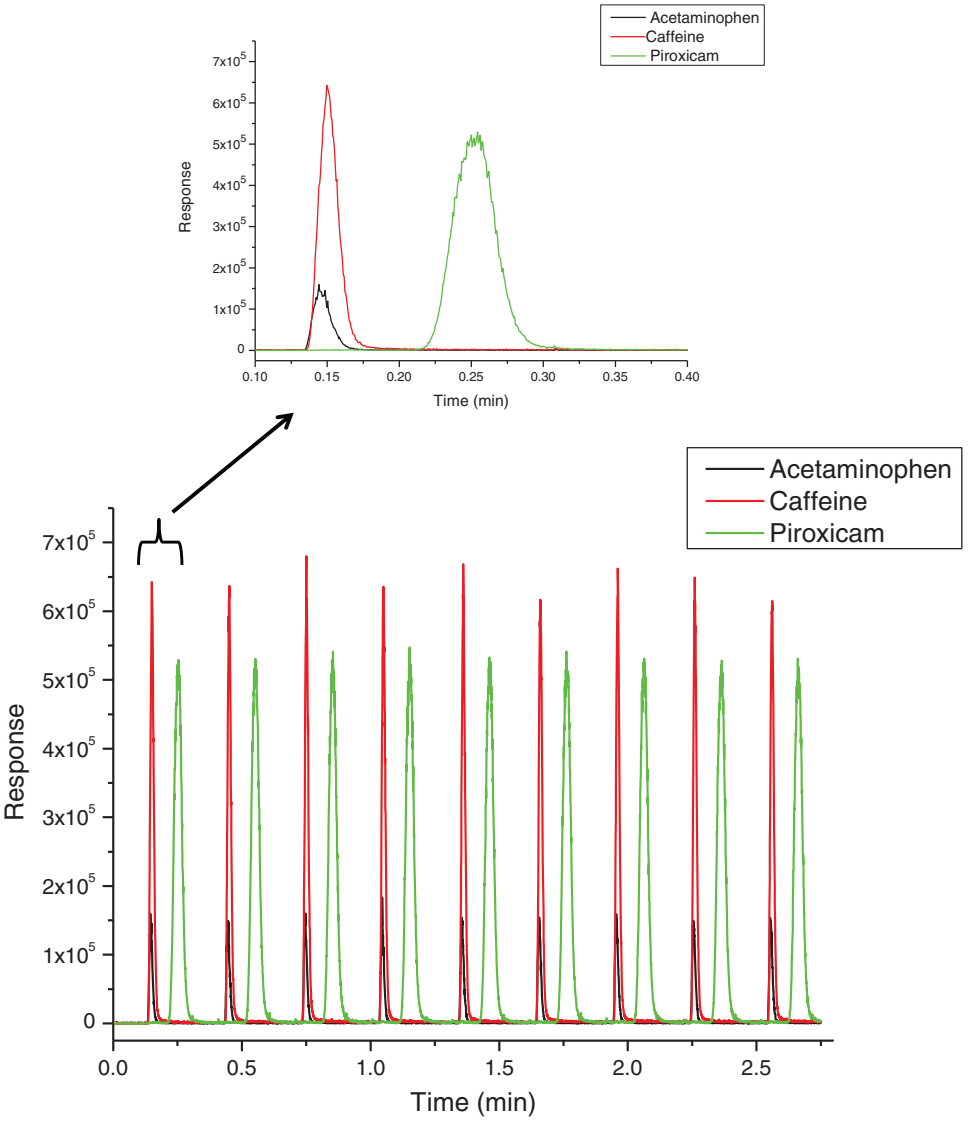

Figure 3.10 The analysis of three pharmaceuticals using pulsed direct injection HPLC–MS. Flow rate, 3.0 ml/min, 40/60 water/methanol mobile phase (0.1% FA). Column 50 mm × 2.1 mm i.d. Hypersil Gold in PSF mode. Outlet segmentation ratio 15% through the column center to MS detector.

3.5 Summary

There have to date been no advances in column technology that are able to provide the benefits of increased sensitivity, efficiency, and speed in a single design

format. Usually, gains in sensitivity come at the cost of speed, since separations need to be run at a flow rate near the minimum in a HETP curve. Curtain flow chromatography, and even PSF chromatography, overcomes this limitation. Likewise, the cost of column efficiency is usually paid for in the currency of time. But AFT columns can provide higher efficiency than conventional columns, especially as the flow rate increases. Hence, the AFT columns function at their best when separations are run fast. Another factor that usually makes the cost of speed too much to bear is the limitation in detection processing, especially if the detector is a mass spectrometer. With AFT columns, less solvent enters the MS, in fact, in direct proportion to the segmentation ratio. Thus, ultrafast, highly efficient, and very sensitive assays can be undertaken using AFT columns with MS detectors.

References

1 Scott, C.D. and Lee, N.E. (1969) *J. Chromatogr.*, **42**, 263–265.
2 Bruns, S., Stoeckel, D., Smarsly, B.M., and Tallarek, U. (2012) *J. Chromatogr.*, **1268**, 53–63.
3 Nawrocki, J., Rigney, M., McCormick, A., and Carr, P.W. (1993) *J. Chromatogr.*, **657**, 229–282.
4 Nawrocki, J., Dunlap, C.A., McCormick, A., and Carr, P.W. (2004) *J. Chromatogr.*, **1028**, 1–30.
5 Yu, H., Jia, C., Wu, H., Song, G., Jin, Y., and Ke, Y., and Liang, X. (2012) *J. Chromatogr.*, **1247**, 63–70.
6 Guiochon, G. (2007) *J. Chromatogr.*, **1168**, 101–168.
7 Eon, C.H. (1978) *J. Chromatogr.*, **149**, 29–42.
8 Knox, J.H. and Parcher, J.F. (1969) *Anal. Chem.*, **41**, 1599–1606.
9 Baur, J.E. and Wightman, R.M. (1989) *J. Chromatogr.*, **482**, 65–73.
10 Farkas, T., Chambers, J.Q., and Guiochon, G. (1994) *J. Chromatogr. A.*, **679**, 231–245.
11 Farkas, T., Sepaniak, M.J., and Guiochon, G. (1996) *J. Chromatogr. A.*, **740**, 169–181.
12 Farkas, T. and Guiochon, G. (1997) *Anal. Chem.*, **69**, 4592–4600.
13 Camenzuli, M., Ritchie, H.J., and Ladine, J.R., and Shalliker, R.A. (2011) *Analyst*, **136**, 5127–5130.
14 Camenzuli, M., Ritchie, H.J., Ladine, J.R., and Shalliker, R.A. (2012) *J. Chromatogr. A*, **1232**, 47–51.
15 Shalliker, R.A., Camenzuli, M., Pereira, L., and Ritchie, H.J. (2012) *J. Chromatogr. A*, **1262**, 64–69.
16 Shalliker, R.A. and Ritchie, H.J. (2014) *J. Chromatogr. A.*, **1335**, 122–135.
17 Shalliker, R.A., Broyles, B.S., and Guiochon, G. (1998) *Am. Lab.*, **30** (21), 124–129.
18 Giddings, J.C. and Robison, R.A. (1962) *Anal. Chem.*, **34**, 885–890.
19 Giddings, J.C. (1963) *Anal. Chem.*, **35**, 1338–1341.
20 Halasz, I. and Heine, E. (1962) *Nature*, **194**, 971.
21 Sternberg, J.C. and Poulson, R.E. (1964) *Anal. Chem.*, **36**, 1492–1502.
22 Jaeger, H.M., Nagel, S.R., and Behringer, R.P. (1996) *Rev. Mod. Phys.*, **68**, 1259–1273.
23 Shalliker, R.A., Broyles, B.S., and Guiochon, G. (2000) *J. Chromatogr. A.*, **878**, 153–163.
24 Wong, V., Shalliker, R.A., and Guiochon, G. (2004) *Anal. Chem.*, **76** (9), 2601–2608.
25 Knox, J.H., Laird, G.R., and Raven, P.A. (1976) *J. Chromatogr.*, **122**, 129–145.
26 Golay, M.J.E. (1961) *Gas Chromatography* (eds H.J. Noebels, R.F. Wall, and N. Brenner), Academic Press, New York, p. 11.
27 Tallarek, U., Baumeister, E., Albert, K., Bayer, E., and Guiochon, G. (1995) *J. Chromatogr. A.*, **696**, 1–18.
28 Van Dusschoten, D., Tallarek, U., Scheenen, T., Neue, U.D., and Van As, H.

(1998) *Mag. Res. Imaging*, **16** (5/6), 703–706.
29 Tallarek, U., Bayer, E., and Guiochon, G. (1998) *J. Am. Chem. Soc.*, **120**, 1494–1505.
30 Tallarek, U., Bayer, E., Van Dusschoten, D., Scheenen, T., Van As, H., Guiochon, G., and Neue, U.D. (1998) *AIChE J.*, **44**, 1962–1975.
31 Shalliker, R.A., Broyles, B.S., and Guiochon, G. (1998) *J. Chromatogr. A.*, **826**, 1–13.
32 Shalliker, R.A., Broyles, B.S., and Guiochon, G. (2000) *J. Chromatogr. A.*, **888**, 1–12.
33 Camenzuli, M., Ritchie, H.J., and Shalliker, R.A. (2013) *Microchem. J.* **110**, 473–479.
34 Camenzuli, M., Ritchie, H.J., Dennis, G.R., and Shalliker, R.A. (2013) *Microchem. J.*, **110**, 726–730.
35 Camenzuli, M., Terry, J.M., Shalliker, R.A., Conlan, X.A., Barnett, N.W., and Francis, P.S. (2013) *Ana. Chim. Acta*, **803**, 154–159.
36 Kocic, D., Pereira, L., Foley, D., Edge, T., Mosely, J.A., Ritchie, H., Conlan, X.A., and Shalliker, R.A. (2013) *J. Chromatogr. A*, **1305**, 102–108.
37 Foley, D., Pereira, L., Camenzuli, M., Edge, T., Ritchie, H., and Shalliker, R.A. (2013) *Microchem. J.*, **110**, 127–132.
38 Catchpoole, H.J., Shalliker, R.A., Dennis, G.R., and Guiochon, G. (2006) *J. Chromatogr. A*, **1117**, 137–145.
39 Broyles, B.S., Shalliker, R.A., and Guiochon, G. (1999) *J. Chromatogr. A.*, **855**, 367–382.
40 Shalliker, R.A., Broyles, B.S., and Guiochon, G. (1999) *J. Chromatogr. A.*, **865**, 83–95.
41 Broyles, B.S., Shalliker, R.A., and Guiochon, G. (2001) *J. Chromatogr. A.*, **917**, 1–22.
42 Gritti, F., Pynt, J., Soliven, A., Dennis, G.R., Shalliker, R.A., and Guiochon, G. (2014) *J. Chromatogr. A.*, **1333**, 32–44.
43 Soliven, A., Foley, D., Pereira, L., Hua, S., Edge, T., Ritchie, H., Dennis, G.R., and Shalliker, R.A. (2014) *Microchem. J.*, **116**, 230–234.